

# Generation of Compliant Mechanisms using Hybrid Genetic Algorithm

Deepak Sharma · Kalyanmoy Deb

Received: date / Accepted: date

**Abstract** Compliant mechanism is a single piece elastic structure which can deform to perform the assigned task. In this paper, the compliant mechanisms are evolved using a constraint based bi-objective optimization formulation which requires one user defined parameter ( $\eta$ ). This user defined parameter limits a gap between a desired path and an actual path traced by the compliant mechanism. The non-linear and discrete optimization problem is solved using the hybrid genetic algorithm (GA) wherein domain specific initialization, two-dimensional crossover operator and repairing techniques are adopted. A bit-wise local search method is used with elitist non-dominated sorting genetic algorithm to further refine the compliant mechanisms. Parallel computations are performed on the master-slave architecture to reduce the computation time. A parametric study is carried out for  $\eta$  value which suggests a range to evolve topologically different compliant mechanisms. The applied and boundary conditions to the compliant mechanisms are considered variables that are evolved by the hybrid GA. The post-analysis of results unveil that the compliant mechanisms are always supported at unique location that can evolve the non-dominated solutions.

**Keywords** Compliant Mechanism · Hybrid Genetic Algorithm · Customization · Local Search · Bi-Objective Optimization

---

D. Sharma  
Department of Mechanical Engineering,  
Indian Institute of Technology Guwahati,  
Assam, India, PIN-781039.  
E-mail: dsharma@iitg.ernet.in

K. Deb  
Electrical and Computer Engineering,  
Michigan State University, East Lansing,  
MI 48824, USA.  
E-mail: kdeb@egr.msu.edu

## 1 Introduction

Topology optimization methodology is commonly used to generate a compliant mechanism in which a flexible structure is designed. This structure can undergo an elastic deformation on the application of applied load. The deformation of elastic structure is then useful to accomplish the assigned task. The field of topology optimization of structure is quite mature by now and has found many applications in product design, off-shore structures, smart structures, microelectromechanical systems [1] etc.

The topology optimization methodology follows continuum mechanics approach in which an optimization procedure decides the optimal distribution of material in a given design domain. There exist methods like homogenization method [2,3], solid isotropic microstructure with penalization method (SIMP) [4], level-set method [5,6], and evolutionary structural optimization (ESO) [7] etc. that are commonly used for topology optimization. These methods are considered computationally efficient in which a discrete optimization problem is simplified into a continuous variable optimization problem. But, the optimal solution will be sensitive towards a threshold value for a continuous design variable.

The major shortcoming of above methods can be eliminated by using Boolean variable (0-1) for material distribution in the design domain. In this scenario genetic algorithm (GA) is a viable approach for topology optimization [8–11]. Moreover, the multiple objectives can be aimed in addition to inherent non-linearity of the optimization problem. The major drawback of GA is a large computation time. But, it can be reduced by performing function evaluations in parallel [12, 13].

The performance of GA can be improved for topology optimization by providing problem-specific modifications [14]. It has been observed that modification at initial population

[15, 16], crossover operator [17], elitist selection strategy [18] and repairing techniques [19] can evolve better offspring solutions in the GA population.

Various formulations have been proposed in the literature to generate the compliant mechanisms. Some of them are minimizing deformation and strain energy using weighted sum method [20], minimizing error of geometric [21] and mechanical advantages [22], maximizing ratio of mutual energy to strain energy [23], maximizing mutual potential energy [24] etc. Most of the above studies combine the multiple objectives into a single objective optimization problem. On the other hand, solving single objective optimization problem as multi-objective optimization can introduce adequate diversity in GA, thereby enhancing the chance of finding good new solutions with generations [12, 25, 26].

From the above discussion, it is clear that GA can be a best tool for generating compliant mechanisms. However, attention is required to modify GA such that the convergence of GA can be improved and better compliant mechanisms can be evolved. This leads to the motivation of present work wherein GA is modified using domain-specific initialization, two-dimensional crossover and repairing techniques. The compliant mechanisms are further refined using a bit-wise local search method. The elitist non-dominated sorting GA (NSGA-II) [27] is used for global search and optimization. The remaining paper is organized in five sections. In Section 2, the problem formulation for the compliant mechanism is presented and the motivation behind user-defined constraints is discussed. In Section 3, the hybrid GA is discussed and modification to NSGA-II are shown. In Section 4, the evolved compliant mechanisms are presented and post analysis of results are done. In Section 5, the paper is concluded and a scope for future work is mentioned.

## 2 Problem Formulation

The bi-objective optimization formulation is presented here in which minimization of weight of the elastic structure is considered as the primary objective. This objective is coupled with the secondary objective in which input energy supplied to the structure is minimized. Both of these objectives are conflicting in nature as the primary objective aims to generate flexible elastic structure and the secondary objective imposes stiffness to the structure. The two objectives for the compliant mechanism is given as

**Minimize:** Weight of the elastic structure,  
**Minimize:** Supplied input energy to the structure. (1)

A continuum mechanics approach is used to evaluate both objectives. In this approach, the design domain as shown in Fig. 1 is represented by the grids. Each grid is either filled with material (black colored grid) or it is a void. By counting number of black grids, the weight of the structure can

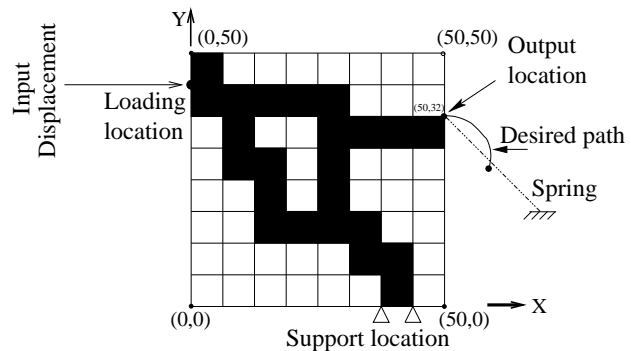


**Fig. 1** A design-domain is represented by square grids, and is subjected to applied and boundary conditions.

be evaluated by multiplying the count with area of grid and density of the material. The input energy supplied to the structure is calculated after performing finite element simulations. It signifies the strain energy stored in the deformed elastic structure and the potential energy stored in the spring as shown in Fig. 1.

The constraints are designed for the path generating compliant mechanism (PGCM) in which a desired path is generated by the elastic structure. In the literature, PGCM is designed by minimizing Euclidean distance between a desired path and an actual path generated by the elastic structure at some fixed points [28]. These fixed points are referred as precision points. In this methodology, a closeness between the paths cannot be ensured and may find a solution generating its actual path far from the desired path. This problem leads to the motivation to develop a formulation wherein constraint is imposed at each precision point such that a gap between the paths can be controlled [12].

A desired path can be represented by the equidistant precision points as shown in Fig. 2. The actual path traced by the elastic structure can also be represented in a similar way. A gap between these paths can be controlled by imposing a limit on each precision point. This is given as

$$d_2 \leq d_1 \quad (2)$$

for each precision point, where  $d_2 (= \sqrt{(x_{ia} - x_i)^2 + (y_{ia} - y_i)^2})$  is Euclidean distance between the precision point ( $i$ ) and the corresponding point ( $ia$ ) of the actual path as shown in Fig. 2. The distance  $d_1 (= \eta \times \sqrt{(x_i - x_{i-1})^2 + (y_i - y_{i-1})^2})$  is  $\eta\%$  of Euclidean distance between the current precision point ( $i$ ) and the previous precision point ( $i - 1$ ).

It can be seen that a gap between the paths is controlled by  $\eta$ . Variation in  $\eta$  value not only will change the optimal solutions, but also it will modify shape and topology of the elastic structure. The effect of different  $\eta$  values is presented in this paper and a suitable range of  $\eta$  is suggested.

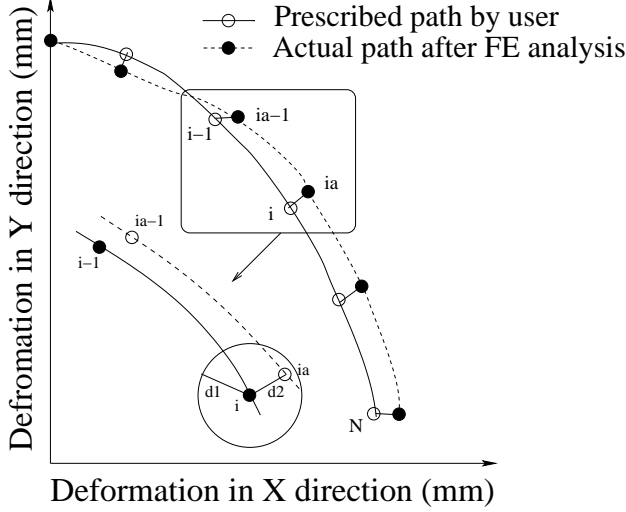


Fig. 2 A prescribed path and an actual path traced by the elastic structure.

Another constraint is also imposed in which the maximum shear stressed developed in the elastic structure should be less than the yield stress of the material which is given as

$$\tau_{max} < \sigma_y. \quad (3)$$

The above constraint bi-objective optimization formulation is used to generate multiple PGCMs. In the next section, the hybrid genetic algorithm is discussed for solving the given optimization problem.

### 3 Hybrid Genetic Algorithm

The hybrid genetic algorithm is used to solve the constraint bi-objective optimization problem of the compliant mechanism. The global search and optimization is done using NSGA-II [27]. This algorithm has successfully been used for structure topology optimization earlier [12, 14, 15, 17, 25].

The flow chart of the hybrid NSGA-II algorithm is shown in Fig. 3. The algorithm starts with random initial population. A domain specific initial population generation strategy is adopted [12] in which the locations of support and applied boundary conditions, and output region are connected to each other. The output region is referred as a point on the elastic structure which will generate a path. It can be seen in Fig. 4 (a), support, loading and output locations are connected by piece-wise linear segments, randomly. These segments can have different length and orientation for different structures in the GA population. In the present example, the support location is connected to the loading location by randomly placing three linear segments. However, these locations are allowed to be connected by two to four linear segments. Similarly any pair of locations can be connected by two to four linear segments. Thereafter, the grids are filled

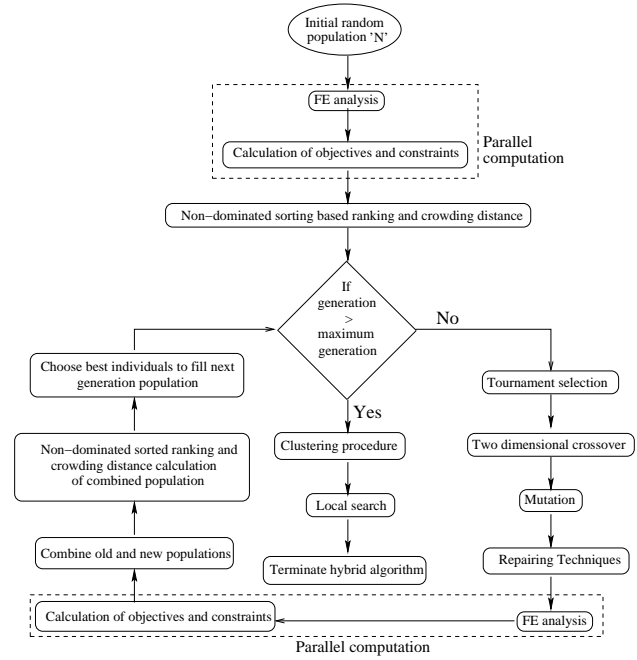


Fig. 3 A flow chart of hybrid NSGA-II algorithm.

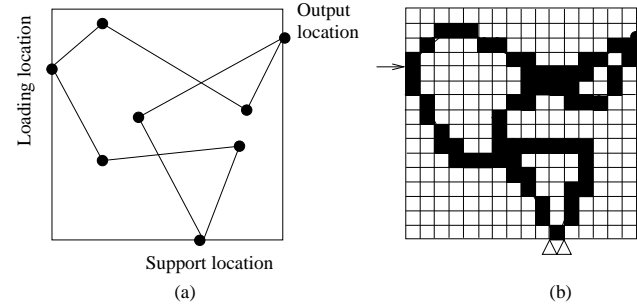


Fig. 4 A domain specific initial population strategy distributes material randomly.

with the material from where these line segments pass. The distribution of material in the design domain can be seen in Fig. 4 (b).

It is worth mentioning that the locations of support and loading conditions are considered as variables. The magnitude of applied boundary condition, that is, input displacement at loading location is also a variable. The support and loading locations are thus different for different individuals in the population. Moreover, these conditions are evolved by the hybrid GA.

Once the initial population is generated, the finite element computations are performed for each elastic structure to calculate the objective and constraints. These computations are done in parallel on the cluster computers using the master-slave architecture. The population is equally divided on the slave processors on which the finite element computations are performed using ANSYS software for each elastic structure.

The rank of each individual in the population is then calculated using non-dominated sorting ranking operator proposed in NSGA-II [27]. The solutions are sorted in different fronts based on the dominance principle. The crowding distance is calculated front wise for each solution. The solutions are then selected using constrained binary tournament selection operator as described in [29]. Here, the solution with better rank and larger crowding distance is selected.

The mating pool is then created after selecting good individuals. The crossover operator is then performed on the population in the mating pool. A two dimensional crossover operator is used in which a block of horizontal or vertical grids are swapped between two randomly selected parent solutions as shown in Fig. 5. The size and location of hori-

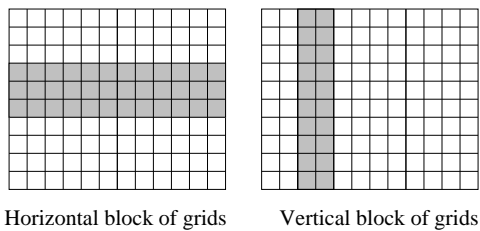


**Fig. 5** A two dimensional crossover that swaps a block of horizontal/vertical block of grids between randomly selected two parent solutions.

zontal/vertical grids are randomly selected within the design domain. Moreover, the swapping of horizontal or vertical block is also decided randomly.

After performing crossover operator the bit-wise mutation operator is used. In this mutation operator each grid is mutation with a probability of  $p_m$ . If the probability condition is satisfied, Boolean variable is mutated to its complement.

The crossover and mutation operators do not respect design feasibility of the elastic structures. In such situation the offspring solution can have disconnected or infeasible geometry as shown in Fig. 6 (a). In this figure a material

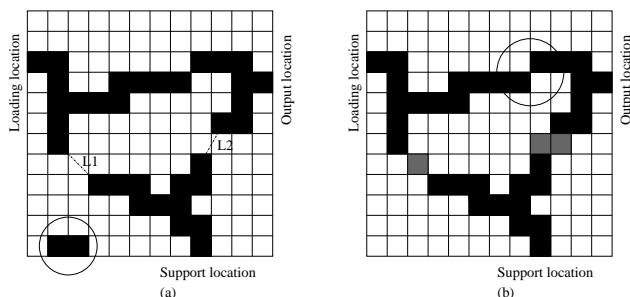


**Fig. 6** The elastic structure with disconnected topology.

discontinuity can be seen among the support, loading and output locations. In this scenario minimum extra material is

placed in the grids to eliminate the problem. It is done by calculating minimum distance between the clusters of material and joined them by a straight line. Thereafter, the material is assigned to those grids where the straight line passes as shown in Fig. 6 (b).

The point singularity is another problem where two grids filled with a material are connected by a point. It is encircled in Fig. 6 (b). A heuristic repairing technique is used in which a point singularity is removed by putting extra material as shown in Fig. 7. In Fig. 7(a), an extra material can be filled

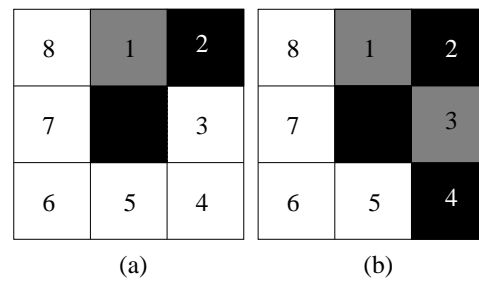


**Fig. 7** Point singularity case is illustrated.

at 1st or 3rd position with an equal probability. In Fig. 7(b), extra material is filled at two grids. Another problem can be seen with a topology in Fig. 6 (a) that few grids with material which are encircled, are not attached to the main topology. In that case, material is removed from those grids as shown in Fig. 6 (b).

The offspring population is generated and is now to be evaluated using parallel computation as described earlier. The rank and crowding distance of each individual are calculated in the combined population from parent and child populations. Here,  $(\mu + \lambda)$  selection scheme is used from evolutionary strategy in which best  $\mu$  solutions are selected from the combined population of  $(\mu + \lambda)$ . Here, the best individuals are selected based on better rank and larger crowding distance. This completes one generation of the hybrid GA. The hybrid GA gets terminated when number of generations reaches maximum allowed generations. The non-dominated solutions evolved by the hybrid GA are stored for clustering and local search.

The clustering procedure is then applied when large number of non-dominated solutions are evolved by the hybrid GA. In this procedure the neighboring solutions (in the objective space) are grouped together using the  $k$ -mean clustering algorithm. One solution from each group of the non-dominated front is chosen as final representative solution. The bit-wise local search method is then executed on the representative solutions.

The local search method uses weighted sum method in which two objectives are added and multiplied by weights as given as

$$\min F(x) = \min \sum_{j=1}^n \frac{\bar{w}_j^x (f_{j_{\max}}^x - f_j^x)}{f_{j_{\max}}^x - f_{j_{\min}}^x}, \quad (4)$$

where  $f_j^x$  is  $j^{\text{th}}$  objective function,  $f_{j_{\min}}^x$  and  $f_{j_{\max}}^x$  are minimum and maximum values of  $j^{\text{th}}$  objective function in the population respectively,  $n$  is number of objectives and  $\bar{w}_j^x$  is the corresponding weight to the  $j^{\text{th}}$  objective function which is computed as

$$\bar{w}_j^x = \frac{(f_{j_{\max}}^x - f_j^x) \setminus (f_{j_{\max}}^x - f_{j_{\min}}^x)}{\sum_{k=0}^M (f_{k_{\max}}^x - f_k^x) \setminus (f_{k_{\max}}^x - f_{k_{\min}}^x)}, \quad (5)$$

where  $M$  is the number of representative solutions after clustering procedure. In (4), the objective function values are normalized to avoid bias towards any objective function. In this approach the weight vector decides the importance of different objectives, in other words it gives the direction to the local search in the objective space. As (5) suggests, these weights are calculated based on their positions in two-objective space after the termination of the hybrid GA.

In the local search method the binary string of the representative solution is converted into a two-dimensional array which is then checked for the grids filled with material. For each grid filled with material, there are eight possible neighborhood cells. One by one all neighboring bits including its own bit value is mutated to its complement. The new elastic structure is then extracted on which the finite element computations are performed for evaluating the objective function and constraints values. If the new structure does not satisfy any of the constraints, the change in the new string is discarded and the old values are restored. Otherwise, the weight of structure represented by the new string is calculated and compared with that of the old string's value. If mutating a bit brings an improvement in the weight objective and the solution remains to be feasible, the change is accepted. Else, the change is discarded and the previous values are restored. When all the bits having a material are mutated along with their neighborhoods, the grids of the new elastic structure are again checked for material and are mutated as discussed above. The local search method is terminated when no change in a bit improves the weight objective value and simultaneously keep the solution feasible. In the same way, all chosen non-dominated solutions are mutated one by one.

## 4 Simulation Results

The material used for generating compliant mechanism is assumed to have Young's modulus ( $E$ ) of 3.3 GPa, yield stress ( $\sigma_y$ ) of 69 MPa, density ( $\rho$ ) of 1.114 gm/cm<sup>3</sup>, and

Poisson's ratio ( $\nu$ ) of 0.40. The displacement boundary condition is applied at the loading location in direction of  $x$ -axis as shown in Fig. 1. Maximum six representative solutions are chosen from the non-dominated set evolved by the hybrid GA using the clustering procedure. A 24-node cluster is used to perform parallel computations. A few GA parameters are kept constant which are given in Table 1. Here, the population size of 240 is used such that sub-population size of 10 can be divided for each salve processor. The crossover probability is kept high to explore the search space by the hybrid GA. However, the mutation probability is kept very low. The generations allowed to the hybrid GA is fixed as 100 so that the non-dominated solutions evolved by the hybrid GA will be further refined by the local search method.

**Table 1** NSGA-II parameters used in this study.

<b>Population</b>	240	<b>Generation</b>	100
<b>Crossover probability</b>	0.95	<b>Mutation probability</b>	1/string length

### 4.1 Parametric Study of $\eta$

The user defined parameter  $\eta$  is responsible to limit a gap between a desired path and an actual path traced by the compliant mechanism. The parametric study of  $\eta$  is done for  $\eta = 5\%$ ,  $10\%$ ,  $15\%$ ,  $20\%$ , and  $25\%$ . For different values of  $\eta$ , the compliant mechanisms generating curvilinear path are evolved.

For  $\eta = 5\%$ , the hybrid algorithm is unable to generate any feasible solution. It is because the feasible space defined by the constraints in (2) is narrow.

When  $\eta = 10\%$  is set, the hybrid GA generates few non-dominated solutions as shown in Fig. 8. Solutions *a* to *f* are generated by NSGA-II. The local search method is then

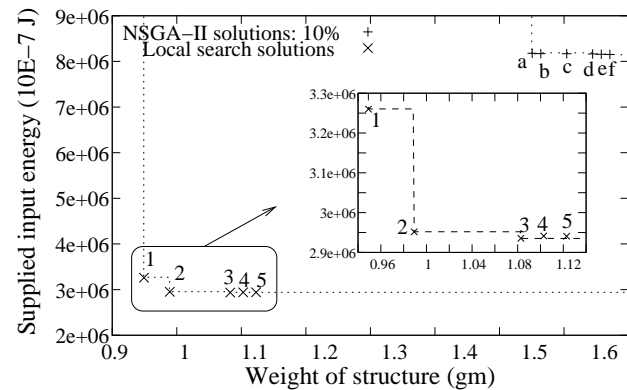


**Fig. 8** The approximate Pareto-optimal solutions evolved by the hybrid algorithm for  $\eta = 10\%$ .

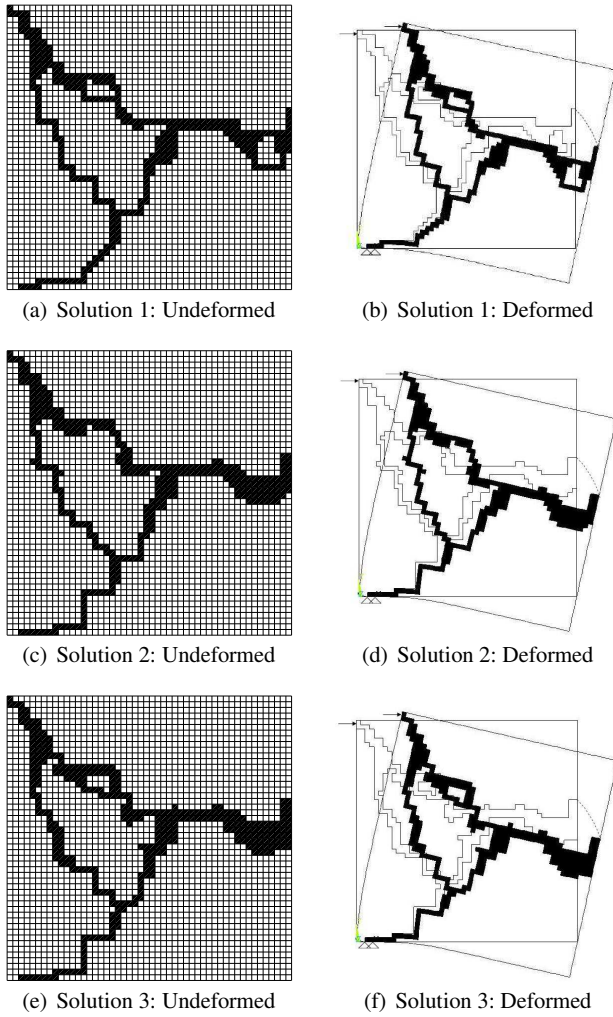


Fig. 9 The compliant mechanisms for  $\eta = 10\%$ .

applied to these solutions which generates five (1 to 5) solutions. Here, solutions *e* and *f* are converged to same solution 5. Among five local search solutions, only three solutions (1, 2 and 3) are non-dominated.

The deformed and undeformed topology of three non-dominated solutions are shown in Fig. 9. In this figure, solution 1 is the minimum weight solution but requires larger input energy to generate the desired curvilinear path. Solution 3 requires minimum supplied input energy but evolves as heavier structure. Solution 2 also shows trade-off between the two-objectives.

For  $\eta = 15\%$ , NSGA-II algorithm evolves five non-dominated solutions (*a* to *e*) as shown in Fig. 10. When local search method is applied on these solutions, solutions (1 to 5) are generated. Among the local search solutions only solutions 1 and 2 are non-dominated.

The topology of solutions 1 and 2 are shown in Fig. 11. These solutions are topologically different and show trade-off between weight and supplied input energy.

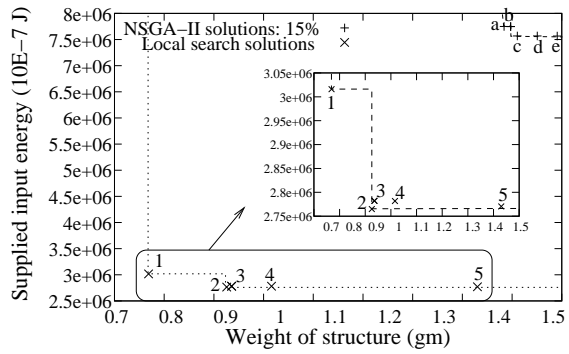


Fig. 10 The approximate Pareto-optimal solutions evolved by the hybrid algorithm for  $\eta = 15\%$ .

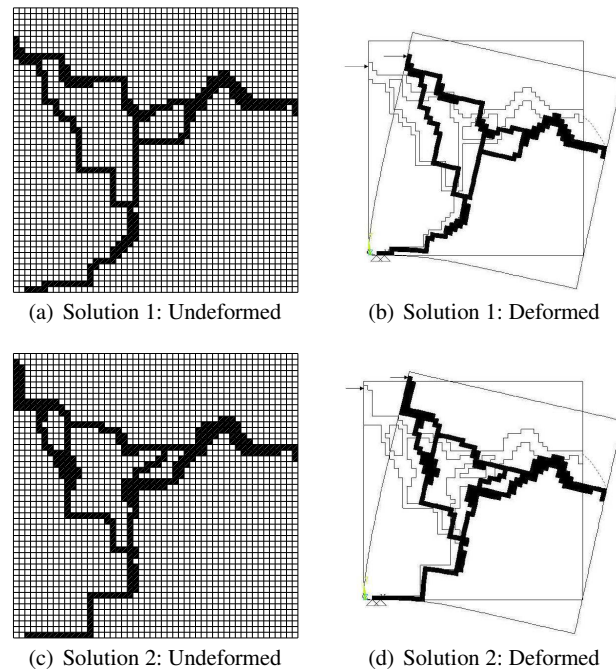
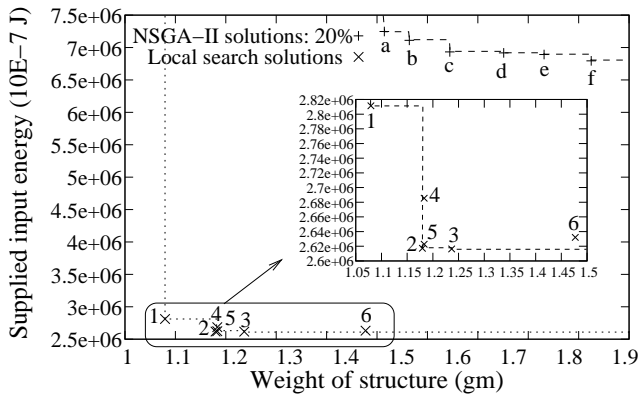


Fig. 11 The compliant mechanisms for  $\eta = 15\%$ .

For  $\eta = 20\%$ , NSGA-II evolves many non-dominated solutions. Among them, six representative solutions (*a* to *f*) are shown in Fig. 12. After the local search, solutions 1 to 6 are generated. But, solutions 1, 2, and 3 are non-dominated.

The deformed and undeformed topologies of solutions 1, 2, and 3 are shown in Fig. 13. It can be seen that solution 3 is topologically different than solutions 1 and 2. All solutions show a large distribution of the material near the center of the design domain.

For  $\eta = 25\%$ , only two solutions are evolved by NSGA-II as shown in Fig. 14 and rest of the population members are same as two solutions. After local search, only solution 1 is non-dominated. The topology of non-dominated solution 1 is shown in Fig. 15. The topology consists of two loops of material.



**Fig. 12** The approximate Pareto-optimal solutions evolved by the hybrid algorithm for  $\eta = 20\%$ .

In Fig. 16, the path traced by the compliant mechanisms are shown for different values of  $\eta$ . It can be observed that the actual path traced by the compliant mechanisms is close to the desired curvilinear path for  $\eta = 10\%$  and  $15\%$ . And also, the actual path intersects the desired path. But, a gap between these two paths increases for higher value of  $\eta$ . A gap between the paths at each precision point is presented in Table 2. It is represented by  $d_1$  and  $d_2$  as defined in (2) in which  $d_1$  represents maximum allowed gap. It can be seen that the precision point 5 is critical where the constraint is active. The gap increases with increase in  $\eta$  value. The above study shows that  $\eta$  ranging from  $10\%$  to  $20\%$  is a suitable where topologically different PGCMS can be evolved and the paths generated by them are close to the desired path.

#### 4.2 Applied and Boundary Conditions

The applied and boundary conditions are considered variables and are evolved by NSGA-II algorithm. These conditions are shown in Table 3 for different values of  $\eta$ . It can be seen that an identical support location is evolved for all compliant mechanisms. This suggests that the present support position is unique for the evolved compliant mechanism to trace the desired curvilinear path or the optimization procedure fails to maintain diversity.

In order to investigate reasons behind the unique support location, the support region is divided into four equal sub-regions as shown in Fig. 17. The support region is located at the bottom of the elastic structure which span from 0 mm to 50 mm. The sub-regions I, II, III and IV span from 0 to 11 mm, 12 to 23 mm, 24 to 35 mm and 36 to 50 mm, respectively.

NSGA-II is run independently for each sub-region in which variable bound for the support location is restricted for one sub-region. Fig. 18 shows the non-dominated solutions evolved for four sub-regions. It can be observed that

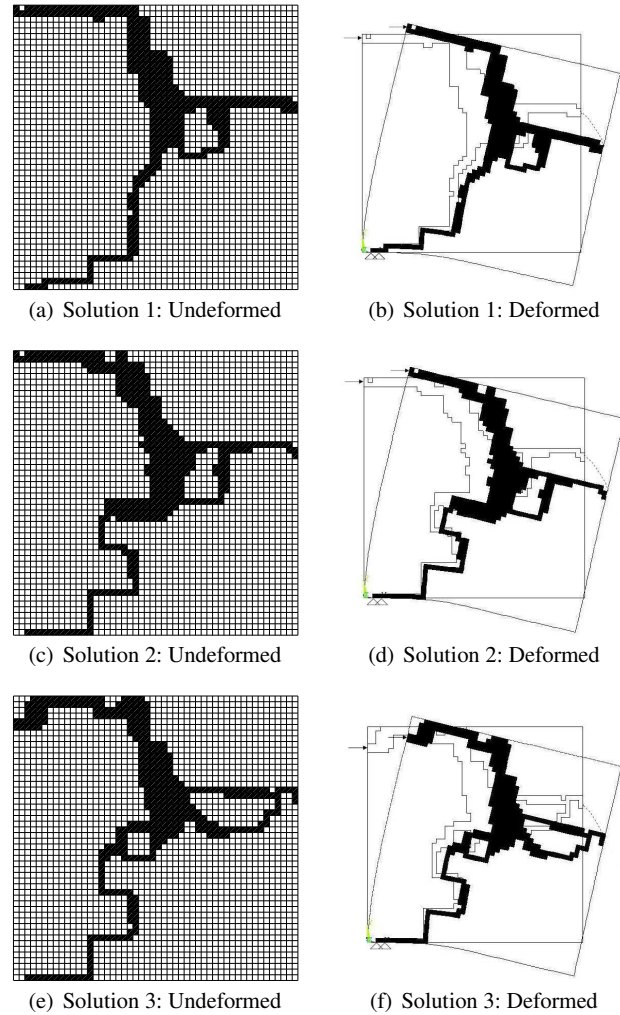


**Fig. 13** The compliant mechanisms for  $\eta = 20\%$ .

the non-dominated solutions evolved from sub-region I dominate rest of the solutions.

The applied and boundary conditions evolved for four sub-regions are shown in Table 4. It can be seen that when the elastic structure is supported away from the origin, it requires more input displacement to generate the desired path. This suggests that more input energy is required to deform the elastic structure. Therefore, the non-dominated solutions evolved in sub-region I dominate other solutions. It signifies that the support location of 2 mm is unique for curvilinear path generating compliant mechanisms.

## 5 Conclusion

In this paper, the parametric study of a constraint bi-objective optimization formulation for the compliant mechanisms was carried out which controlled a gap between the desired path and the actual path. The study suggested that  $\eta$  can be var-

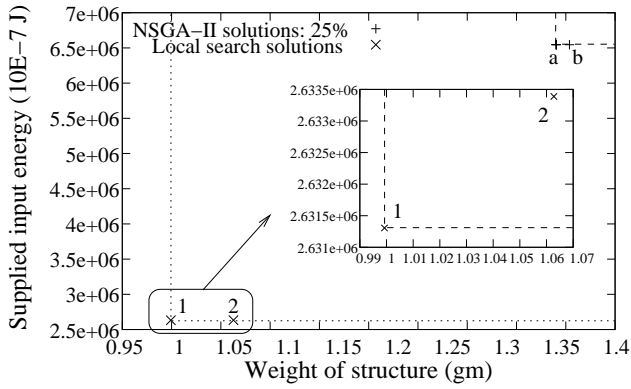


**Fig. 14** An approximate Pareto-optimal solution evolved by the hybrid algorithm for  $\eta = 25\%$ .

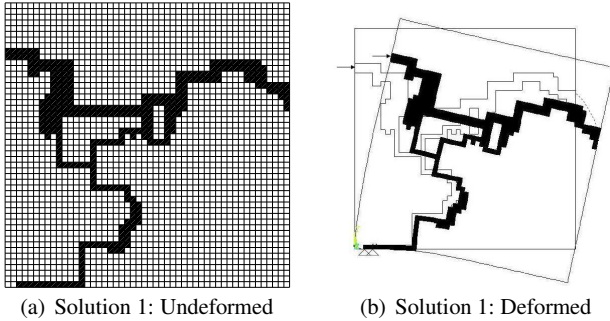
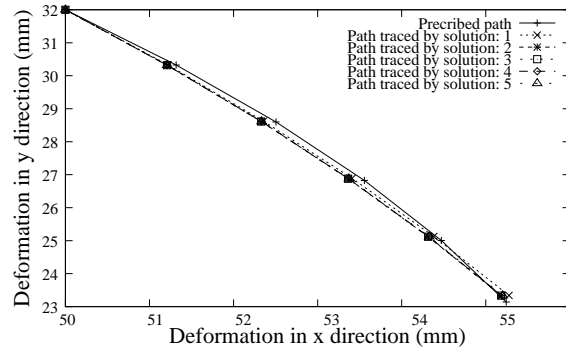


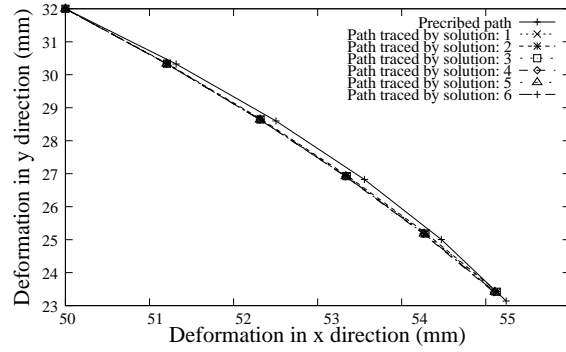
**Fig. 15** The topology of compliant mechanism for  $\eta = 25\%$ .

**Table 2** The position of the precision points on the desired path and the corresponding point on the actual path traced by the compliant mechanisms for different values of  $\eta$ .

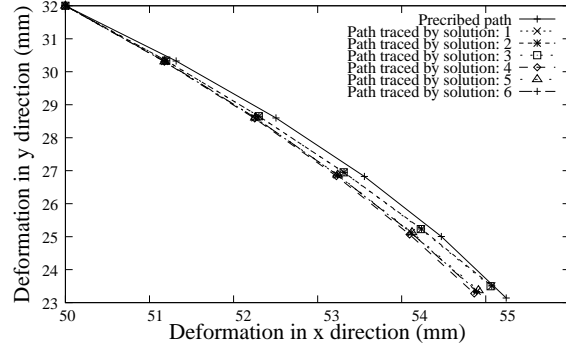
Precision points	1	2	3	4	5
For $\eta = 10\%$					
$d_1$	0.213	0.209	0.206	0.204	0.202
Sol. 1: $d_2$	0.096	0.149	0.160	0.153	0.202
Sol. 2: $d_2$	0.108	0.174	0.198	0.192	0.202
Sol. 3: $d_2$	0.109	0.176	0.201	0.195	0.202
For $\eta = 15\%$					
$d_1$	0.320	0.314	0.309	0.306	0.303
Sol. 1: $d_2$	0.112	0.191	0.239	0.268	0.303
Sol. 2: $d_2$	0.111	0.189	0.236	0.266	0.303
For $\eta = 20\%$					
$d_1$	0.426	0.419	0.412	0.408	0.404
Sol. 1: $d_2$	0.139	0.249	0.326	0.377	0.404
Sol. 2: $d_2$	0.118	0.208	0.272	0.329	0.404
Sol. 3: $d_2$	0.119	0.210	0.277	0.334	0.404
For $\eta = 25\%$					
$d_1$	0.533	0.524	0.516	0.510	0.505
Sol. 1: $d_2$	0.141	0.260	0.357	0.437	0.505



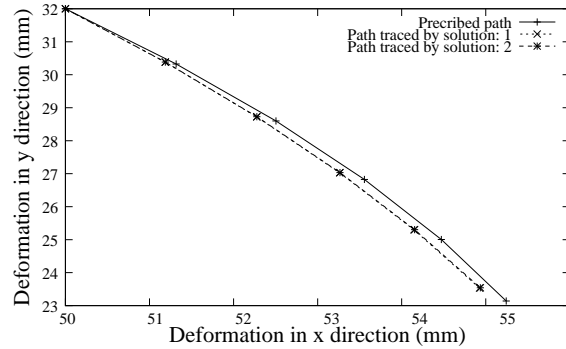
(a) For  $\eta = 10\%$



(b) For  $\eta = 15\%$



(c) For  $\eta = 20\%$



(d) For  $\eta = 25\%$

**Fig. 16** The desired curvilinear path and the actual path traced by the compliant mechanisms.

**Table 3** Applied and boundary conditions of evolved compliant mechanisms for different values of  $\eta$ .

Conditions	Location from origin
For $\eta = 10\%$	
Support position	2 mm
Loading position	48 mm
Input displacement magnitude	10 mm
For $\eta = 15\%$	
Support position	2 mm
Loading position	48 mm and 46 mm
Input displacement magnitude	10 mm and 9 mm
For $\eta = 20\%$	
Support position	2 mm
Loading position	48 mm
Input displacement magnitude	10 mm
For $\eta = 25\%$	
Support position	2 mm
Loading position	40 mm
Input displacement magnitude	8 mm

**Table 4** Applied and boundary conditions of evolved compliant mechanisms for four sub-regions.

Conditions	Location from origin
For region I	
Support position	2 mm
Input displacement magnitude	7 mm
For region II	
Support position	12 mm
Input displacement magnitude	10 mm
For region III	
Support position	24 mm
Input displacement magnitude	12 mm
For region IV	
Support position	36 mm
Input displacement magnitude	14 mm

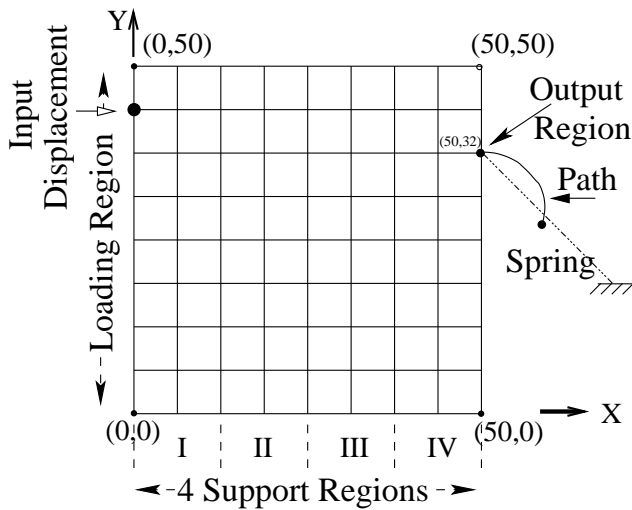


**Fig. 17** The support region of a design domain is divided into four sub-regions.

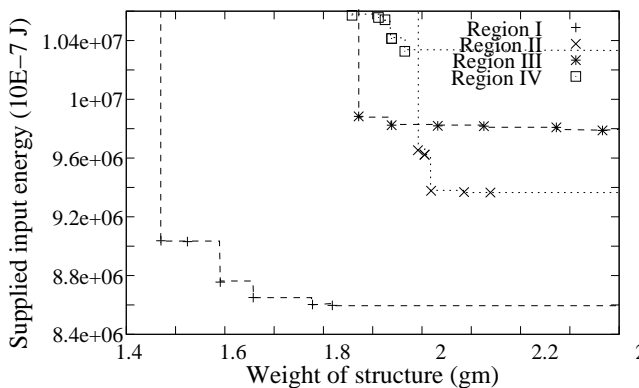


**Fig. 18** A comparison between the NSGA-II solutions evolved from different sub-region analyses.

ied between 10% to 20% to evolve topologically different PGCMs. This range of  $\eta$  kept the actual path generated by the compliant mechanisms closer to the desired curvilinear path. Genetic algorithm was modified using domain specific initialization, two-dimensional crossover operator and repairing techniques. These modification helped NSGA-II to evolve a set of non-dominated solutions. These solutions were further refined using a bit-wise local search method which generated smooth structures. Moreover, the support and applied boundary conditions were evolved by the hybrid GA in which all elastic structure were supported at the identical location. This location was unique for evolving the non-dominated PGCMs. This fact was supported by region-wise analysis of the support region. In the future, the same formulation and the hybrid algorithm can be used to evolve the compliant mechanisms which can trace variety of paths. Further attention is required to modify GA so that a diverse set of non-dominated solutions can be evolved.

## References

1. G. K. Ananthasuresh. *Optimal Synthesis Methods for MEMS*. Kluwer Academic Publishers, 2003.
2. M. P. Bendsøe and N. Kikuchi. Generating optimal topologies in structural design using a homogenization method. *Computer Methods in Applied Mechanics and Engineering*, 71:197–224, 1988.
3. S. Nishiwaki, M. I. Frecker, S. Min, and N. Kikuchi. Topology Optimization of Compliant Mechanisms using the Homogenization Method. *International Journal for Numerical Methods in Engineering*, 42(3):535–559, 1998.
4. M. P. Bendsøe. Optimal Shape Design as a Material Distribution Problem. *Structural and Multidisciplinary Optimization*, 1(4):193–202, 1989.
5. J. A. Sethian and Andreas Wiegmann. Structural boundary design via level set and immersed interface methods. *Journal of Computational Physics*, 163(2):489–528, 2000.
6. Michael Yu Wang, Xiaoming Wang, and Dongming Guo. A Level Set Method for Structural Topology Optimization. *Computer Methods in Applied Mechanics and Engineering*, 192(1–2):227–246, 2003.

7. Y. M. Xie and G. P. Steven. A Simple Evolutionary Procedure for Structural Optimization. *Computers & Structures*, 49(5):885–896, 1993.
8. C. D. Chapman, K. Saitou, and M. J. Jakiela. Genetic Algorithms as an Approach to Configuration and Topology Design. *ASME, Journal of Mechanical Design*, 116(4):1005–1012, December 1994.
9. C. D. Chapman and M. J. Jakiela. Genetic algorithm-based structural topology design with compliance and topology simplification considerations. *ASME, Journal of Mechanical Design*, 118:89–98, March 1996.
10. J. W. Duda and M. J. Jakiela. Generation and classification of structural topologies with genetic algorithm speciation. *ASME, Journal of Mechanical Design*, 119:127–131, March 1997.
11. M. J. Jakiela, C. D. Chapman, J. Duda, A. Adewuya, and K. Saitou. Continuum structural topology design with genetic algorithms. *Computer Methods in Applied Mechanics and Engineering*, 186:339–356, March 2000.
12. Deepak Sharma, Kalyanmoy Deb, and N. N. Kishore. Domain-Specific Initial Population Strategy for Compliant Mechanisms using Customized Genetic Algorithm. *Structural and Multidisciplinary Optimization*, 43(4):541–554, April 2011.
13. Lingyun Wei, Tianbing Tang, Xianghong Xie, and Wenjie Shen. Truss optimization on shape and sizing with frequency constraints based on parallel genetic algorithm. *Structural and Multidisciplinary Optimization*, 43(5):665–682, 2011.
14. D. Sharma, K. Deb, and N.N. Kishore. Towards Generating Diverse Topologies of Path Tracing Compliant Mechanisms using a Local Search Based Multi-Objective Genetic Algorithm Procedure. In *Evolutionary Computation, 2008. CEC 2008. (IEEE World Congress on Computational Intelligence). IEEE Congress on*, pages 2004–2011. IEEE, june 2008.
15. Deepak Sharma, Kalyanmoy Deb, and N. N. Kishore. An improved initial population strategy for compliant mechanism designs using evolutionary optimization. In *ASME International Design Engineering Technical Conferences (IDETC) and Computers and Information in Engineering Conference (CIE), New York, USA*, pages Paper No. DETC2008–49187, August 3-6 2008.
16. Hyunjin Shin and Akira Todoroki. Elite-initial population for efficient topology optimization using multiobjective genetic algorithms. *International Journal of Aeronautical and Space Sciences*, 14(4):324–333, 2013.
17. Deepak Sharma, Kalyanmoy Deb, and N. N. Kishore. A Domain-Specific Crossover and a Helper Objective for Generating Minimum Weight Compliant Mechanisms. In *Proceedings of the 10th annual conference on Genetic and evolutionary computation*, GECCO '08, pages 1723–1724, New York, NY, USA, 2008. ACM.
18. Dongfang Li, Shenyan Chen, and Hai Huang. Improved genetic algorithm with two-level approximation for truss topology optimization. *Structural and Multidisciplinary Optimization*, pages 1–20, 2013.
19. B. Xu, J.P. Ou, and J.S. Jiang. Integrated optimization of structural topology and control for piezoelectric smart plate based on genetic algorithm. *Finite Elements in Analysis and Design*, 64(0):1 – 12, 2013.
20. G. K. Ananthasuresh, S. Kota, and N. Kikuchi. Strategies for systematic synthesis of compliant mems. In *Proceedings of the 1994 ASME Winter Annual Meeting*, pages 677–686, November 1994.
21. O. Sigmund. On the Design of Compliant Mechanisms using Topology Optimization. *Mechanics Based Design of Structures and Machines*, 25(4):493–524, 1997.
22. U. D. Larsen, O. Sigmund, and S. Bouwstra. Design and Fabrication of Compliant Micromechanisms and Structures with Negative Poisson's Ratio. *Journal of Microelectromechanical Systems*, 6(2):99–106, June 1997.
23. M. I. Frecker, G. K. Ananthasuresh, S. Nishiwaki, N. Kikuchi, and S. Kota. Topological Synthesis of Compliant Mechanisms using Multi-Criteria Optimization. *ASME, Journal of Mechanical Design*, 119(2):238–245, June 1997.
24. Kerr-Jia Lu and S. Kota. Topology and Dimensional Synthesis of Compliant Mechanisms using Discrete Optimization. *ASME, Journal of Mechanical Design*, 128(5):1080–1091, September 2006.
25. Deepak Sharma, Kalyanmoy Deb, and N. N. Kishore. Customized evolutionary optimization procedure for generating minimum weight compliant mechanisms. *Engineering Optimization*, 46(1):39–60, 2014.
26. N.P. Garcia-Lopez, M. Sanchez-Silva, A.L. Medaglia, and A. Chateauneuf. An improved robust topology optimization approach using multiobjective evolutionary algorithms. *Computers & Structures*, 125(0):1 – 10, 2013.
27. K. Deb, A. Pratap, S. Agarwal, and T. Meyarivan. A Fast and Elitist Multiobjective Genetic Algorithm: NSGA-II. *Evolutionary Computation, IEEE Transactions on*, 6(2):182 –197, apr 2002.
28. K. Tai, G. Y. Cui, and T. Ray. Design Synthesis of Path Generating Compliant Mechanisms by Evolutionary Optimization of Topology and Shape. *ASME, Journal of Mechanical Design*, 124(3):492–500, September 2002.
29. Kalyanmoy Deb. An efficient constraint handling method for genetic algorithms. *Computer Methods in Applied Mechanics and Engineering*, 186(2-4):311–338, 2000.